GFZ
Helmholtz-Zentrum
POTSDAM

Originally published as:

Key Points:
- Following the X6.9 solar flare event of 9 August 2011, negative crochets were observed at dayside equatorial stations
- Global ionospheric current system due to the solar flare that cannot be explained by an enhancement of the background Sq current system
- Contribution from the D-region currents is suspected for the changes of the global ionospheric system

Supporting Information:
- Table S1

Correspondence to:
N. S. A. Hamid,
shazana.ukm@gmail.com

Investigation of Unusual Solar Flare Effect on the Global Ionospheric Current System

N. M. N. Annadurai[1] (iD)**, N. S. A. Hamid[1,2]** (iD)**, Y. Yamazaki[3]** (iD)**, and A. Yoshikawa[4,5]** (iD)

[1]School of Applied Physics, Faculty of Science and Technology, Universiti Kebangsaan Malaysia, Bangi, Malaysia, [2]Space Science Centre (ANGKASA), Institute of Climate Change, Universiti Kebangsaan Malaysia, Bangi, Malaysia, [3]GFZ German Research Centre for Geosciences, Potsdam, Germany, [4]Department of Earth and Planetary Sciences, Faculty of Sciences, Kyushu University, Fukuoka, Japan, [5]International Center for Space Weather Science and Education, Kyushu University, Fukuoka, Japan

Abstract In this paper, we present our investigation of geomagnetic crochets observed following the X-class solar flare events on 9 August 2011 (X6.9) and 24 September 2011 (X1.4). Both events occurred during geomagnetically quiet times (Kp ≤ 3). The analysis of the geomagnetic crochets near the magnetic equator revealed very different responses in the ionospheric currents between these two events. During the 9 August 2011 event, a reduction of the eastward equatorial electrojet was observed in all daytime stations studied, while the daytime eastward equatorial electrojet was observed to enhance during the 24 September 2011 event. A spherical harmonic analysis was applied to the observations from nearly 160 ground stations at middle and low latitudes to derive the equivalent ionospheric current system for the geomagnetic crochets as well as background solar-quiet (Sq) variations for both events. The equivalent current system of the geomagnetic crochets for the 24 September 2011 event showed a similar pattern with the background Sq current system and thus can be attributed to the enhancement of Sq currents. However, the crochet current system for the 9 August 2011 event revealed a different pattern from the background Sq current system in both Northern and Southern Hemispheres. It is suggested that unusual geomagnetic crochets during the 9 August 2011 event may be dominated by the ionospheric currents at D-region altitudes.

1. Introduction

A solar flare is an eruption of electromagnetic waves from the Sun. The phenomenon is sometimes accompanied by short-lived geomagnetic disturbances called geomagnetic *crochets* or *solar flare effects* (SFEs), which can be detected by ground-based magnetometers mostly on the sunlit side of the Earth (Annadurai et al., 2018; Campbell, 2003; Yamazaki & Maute, 2017). It is believed that SFEs are associated with ionospheric currents in the E-region ionosphere (90–150 km), which are altered during the flare due to the enhanced ionization caused by X-ray and EUV radiation.

When solar disturbances are absent, the E-region currents at middle and low latitudes are dominated by the solar-quiet (Sq) current system (e.g., Chulliat et al., 2016; Yamazaki et al., 2011), which results from the ionospheric wind dynamo process (e.g., Richmond, 1995; Richmond & Maute, 2014). According to the dynamo theory, the current density **J** can be expressed as follows: $\mathbf{J} = \boldsymbol{\sigma} \cdot (\mathbf{E} + \mathbf{U} \times \mathbf{B})$, where $\boldsymbol{\sigma}$ is the ionospheric conductivity tensor, **E** is the electric field, **U** is the neutral wind, and **B** is the Earth's main magnetic field. The ionospheric conductivity $\boldsymbol{\sigma}$ depends strongly on the plasma density of the ionosphere, which enhances during solar flares (e.g., Thome & Wagner, 1971).

Early studies attributed geomagnetic crochets to a simple enhancement of the background Sq currents (e.g., McNish, 1937) based on the fact that the equivalent ionospheric current systems for Sq and SFE are similar in shape. The equivalent Sq current system usually consists of two large-scale current vortices on the dayside ionosphere; a counterclockwise vortex is in the Northern Hemisphere and a clockwise vortex in the Southern Hemisphere (e.g., Matsushita, 1965). The equivalent SFE current system has generally the same pattern as the Sq current system, as previous studies have shown (Curto et al., 1994; Gaya-Piqué et al., 2008; Van Sabben, 1961, 1968; Veldkamp & Van Sabben, 1960; Yasuhara & Maeda, 1961). These studies, however, also pointed out that the locations of the SFE current foci are often displaced from those of the Sq current system. The discrepancies between SFE and Sq current systems were considered to be due to contributions from different heights. That is, the Sq currents mainly flow in the E region, while SFE currents may extend into the D

region (below 90 km). For instance, Richmond and Venkateswaran (1971) showed that the X-ray in the 2–10-Å range, which enhances during solar flares, is effective in ionizing the region at 80–100-km altitude.

Near the magnetic equator (approximately $+/-3°$ from the magnetic equator), the E-region currents are enhanced due to the so-called Cowling effect (Baker & Martyn, 1953; Hirono, 1950). The enhanced eastward current flows along the magnetic equator is referred to as the equatorial electrojet (EEJ; Chapman, 1951). Nagata (1952) reported that the amplitude of SFE in the horizontal (H) component of the geomagnetic field at Huancayo, Peru, was enhanced due to the presence of the EEJ. Rastogi et al. (1999) established that SFE (H) at the magnetic equator is positive and negative during the periods of normal (eastward) and reversed (westward) EEJ, respectively. Yamazaki et al. (2009), and later Rastogi et al. (2013), studied unusual SFE events observed on 18 June 2000 and 3 July 2002. During these events, SFEs in H near the magnetic equator were negative in the midday sector around 10:30–13:00 LT despite positive Sq (H). Yamazaki et al. (2009) called such counter-Sq SFEs near the magnetic equator SFE*s. Sripati et al. (2013) studied the response of the low-latitude ionosphere to the X-class solar flare event on 9 August 2011, using various ground measurements. The H-component magnetic data at Tirunelveli, India, revealed the occurrence of SFE*.

The present study also examines the ionospheric response during the solar flare event of 9 August 2011. The aim of the study is to reveal, for the first time, the global ionospheric current system associated with SFE*. This is made possible by using ground-based magnetometer data from approximately 160 stations worldwide. The uniqueness of this event is demonstrated by comparing the results with those from another X-class solar flare event on 24 September 2011.

2. Data Sets and Methodology

We utilize ground-based magnetometer data in the range of $+/-60°$ magnetic latitude to study the solar flare influence on the global ionospheric current system. Higher latitude stations were excluded in order to avoid contamination from polar-region currents that are generated by solar wind-magnetosphere dynamo (Matsushita & Xu, 1982; Weimer, 2013). Total number of stations used in this study is 155. Vector magnetometer data were obtained from various magnetometer networks such as MAGnetic Data Acquisition System/Circum-pan Pacific Magnetometer Network (Hamid et al., 2014; Yumoto, 2006), International Real-time Magnetic Observatory Network (Love & Chulliat, 2013), Southeast Asia Low-Latitude Ionospheric Network (Maruyama et al., 2007), World Data Centre for Geomagnetism, Edinburgh, Low-Latitude Ionospheric Sensor Network, Geospatial Information Authority of Japan, SuperMAG (Gjerloev, 2009, 2012), Deutsches GeoForschungsZentrum, Ocean Hemisphere Network Porject (Shimizu & Utada, 1999), and West African Magnetometer NETwork (Alken et al., 2013). The distribution of magnetometer stations is shown in Figure 1, while information of each station including the geographic coordinates and quasi-dipole coordinates is presented in supporting information Table S1. Quasi-dipole coordinates are magnetic coordinates that are used in the spherical harmonic analysis (SHA). All the magnetometer data are expressed in the magnetic-northward (N), magnetic-eastward (E), and vertical (Z) components using local magnetic coordinates (e.g., Laundal & Richmond, 2017).

The onset and peak times of SFE/SFE* are determined based on the N-component magnetic field at an equatorial station where the geomagnetic crochet is most prominent. At each station, the amplitude of SFE/SFE* was derived as the difference of the magnetic field at the onset and peak times for each component. We also derived the amplitude of Sq as the difference between the magnetic field at the SFE/SFE* onset time and the average nighttime value during 22:00–02:00 LT. Although there are several approaches to evaluate Sq variation (e.g., Rahim & Kumbher, 2016), we adopted this present simple method used in most of previous studies in this area (e.g., Curto et al., 1994; Rastogi et al., 2013; and many others).

A SHA was performed to determine the equivalent ionospheric current system for SFE/SFE* as well as Sq. The methodology follows that detailed by Yamazaki and Maute (2017). Equivalent ionospheric current systems at 110 km were derived using the spherical harmonics of up to degree $n = 5$, which is sufficient to resolve large-scale structure of the current system (Takeda, 1999, 2002). The calculations were made both including and excluding the equatorial stations within $+/-3°$ from the magnetic equator. Since the patterns of the current system were largely the same for the two cases, we show the results including the equatorial stations.
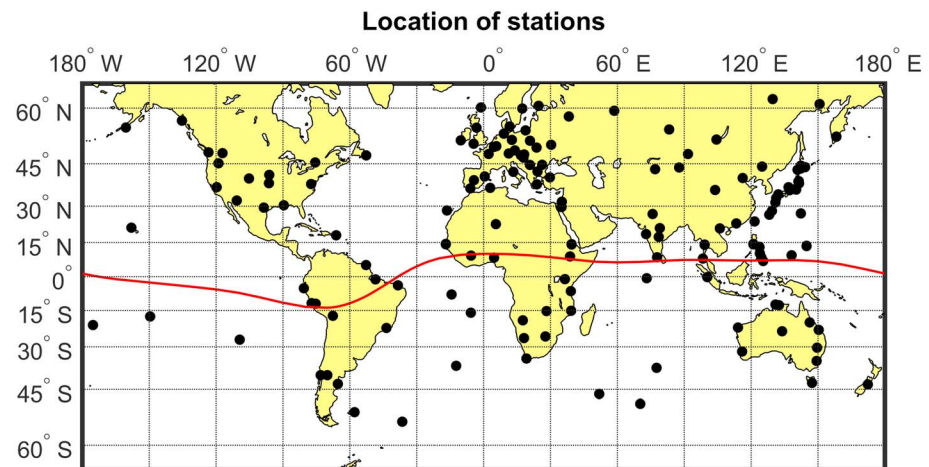
Figure 1. Magnetometer stations used in this study denoted by the black dots. The red line across the map is the magnetic equator.

In addition to the geomagnetic field data, we also use the solar X-ray intensity obtained from Geostationary Operational Environmental Satellites and the geomagnetic activity index Kp.

3. Results and Discussions

3.1. Solar X-Ray and Geomagnetic Activity

We examined geomagnetic crochets observed during 2008–2014. The investigation was made using the N-component magnetic field data from equatorial stations during the solar flare events listed in the solar event archive at the Lockheed Martin Solar and Astrophysics Laboratory. From our analysis, we have identified only one solar flare event that caused SFE*. The rareness of SFE* was also noted by previous researchers (Rastogi et al., 2013; Yamazaki et al., 2009). The event occurred following the X-class solar flare on 9 August 2011 that erupted from AR#11263 (17°N, 69°W) at 07:48 UT and lasted for ~ 20 min. The plot of X-ray flux, SYM-H index, and Kp index for this event are depicted in Figures 2a, 2b, and 2c, respectively. The blue and red lines in Figure 2a indicate the intensity of X-ray at 1.0–8.0 Å and 0.5–3.0 Å, respectively. The flare class (A, B, C, M, and X) is also indicated at the right side of Figure 2a. The 9 August 2011 solar flare occurred during the recovery phase of geomagnetic storm that started at the night of 5 August 2011 (not shown here). The low SYM-H values on 9 August 2011 (Figure 2b) are due to the ring current developed during the solar storm. Although the storm effect known as the disturbance dynamo sometimes perseveres over a day, it is not likely that the disturbance of zonal electric field lasts for 3 days (Huang et al., 2005). Thus, the contribution of the 5 August 2011 geomagnetic storm to our SFE* results can be discounted. This is agreeable with Kp indices in Figure 2c that represent the X6.9 solar flare event took place during the period of low geomagnetic activity (Kp ~ 3) day.

For the purpose of comparison, we have also analyzed geomagnetic crochets during another X-class (X1.6) solar flare event that occurred on 24 September 2011. This solar flare erupted from AR#1302 (13°N, 61°E) at 09:21 UT and lasted for 27 min. Figures 3a, 3b, and 3c illustrate the X-ray intensity, SYM-H index, and Kp index, respectively, for this event. Similar with the August event, the geomagnetic activity was also low during the 24 September 2011 solar flare event (positive SYM-H variation and Kp < 2).

Equatorial geomagnetic field data in the N component for 9 August 2011 are presented in Figure 4a, along with the X-ray intensity. The red-dashed line indicates the onset time (08:02 UT). Figure 4b displays the amplitude of SFE/SFE*(ΔN) and the local time for each equatorial station. The stations are Koror (KOR), Phuket (PKT), Adis Ababa (AAB), Tirunelveli (TIR), Davao (DAV), Yap Island (YAP), Tatuoca (TTB), and Huancayo (HUA). Negative crochets in N were observed at all the equatorial stations on the sunlit side during the event, corresponding to the westward ionospheric currents induced by the solar flare. The largest SFE was detected at KOR with the amplitude of −50.40 nT followed by PKT with the amplitude of −33.30 nT. KOR was located in the morning sector, where the EEJ is relatively weak and occasionally turns westward, which is known as
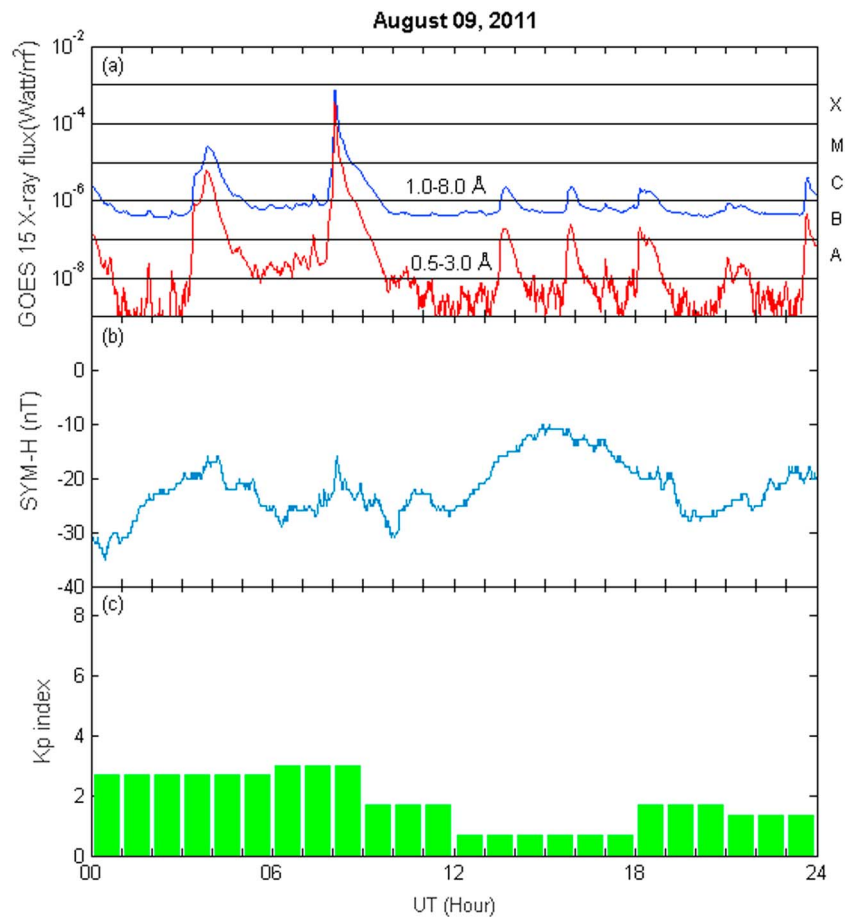
Figure 2. (a) Solar X-ray intensity, (b) SYM-H index, and (c) Kp index on 9 August 2011.

counter electrojet, or CEJ (Marriott et al., 1979; Mayaud, 1977; Rastogi, 1974). Sq (N) at KOR was −4.7 nT, which indicates the occurrence of a weak CEJ. Negative crochets are often observed during CEJ events (Rastogi et al., 1975; Sastri, 1975). At other dayside equatorial stations (i.e., AAB, TIR, PKT, DAV, and YAP), however, Sq (H) was positive. Thus, the negative crochets observed at those stations are SFE*. The amplitude of SFE is very small at TTB and HUA, which were located on the night side. In addition, the responses of some off-equatorial magnetometer data were already reported by Sripati et al. (2013).

The results for the second event, which occurred on 24 September 2011, are summarized in Figures 4c and 4d. The onset of SFE was at 09:35 UT. The positive SFEs (N) observed at dayside stations indicate the enhancement of the eastward EEJ, with the strongest effect at AAB at 12:01 LT with the amplitude of 30.68 nT. Positive SFEs were also recorded at KOR, TIR, and PKT with the amplitude of 24.33, 16.46, and 18.80 nT, respectively. A negative SFE (N) was observed at TTB during a CEJ event. Sq (N) at TTB was −18.20 nT. The SFE amplitudes were very small in the dusk sector at DAV and YAP and on the night side at HUA. SFEs observed at equatorial stations during this event are consistent with the previous results by Rastogi et al. (1999). That is, Sq (N) is positive and negative during the normal and reversed EEJ, respectively.

To further see the differences in the ionospheric response during these two solar flare events, we perform a SHA, using magnetometer data from the stations listed in Table S1. This provides us with the overview picture of the global ionospheric current system associated with SFE/SFE* as well as Sq.

3.2. SHA

The equivalent ionospheric current systems derived using SHA are shown in Figures 5, 6, 7, and 8. The results of the SHA in Figure 5 illustrate the global structure of the ionospheric current systems for Sq and Figure 6 for SFE on 9 August 2011. The green and light blue contours correspond to positive and negative parts of the
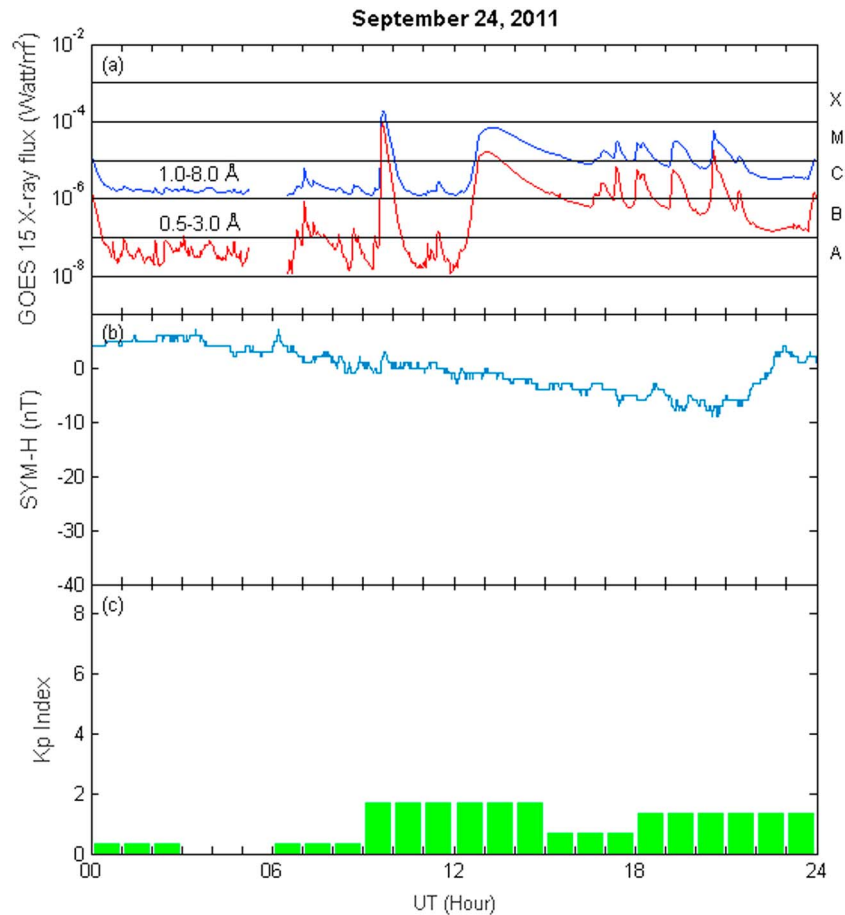
Figure 3. Same as Figure 2 but for 24 September 2011.

current functions, respectively. Contour intervals are 20 and 10 kA for the Sq and SFE/SFE* current systems, respectively. The uncertainty was evaluated for the equivalent current systems by calculating the standard deviation (σ) of the current function using the bootstrap technique. In general, σ is small on the night side and is largest at midlatitudes on the dayside. The maximum value of σ is indicated at the right corner of each panel. The arrows represent horizontal magnetic field perturbations due to Sq and SFE, which are rotated 90° clockwise to indicate the direction of equivalent currents. The orange line shows the magnetic equator, while the blue lines indicate $+/-60°$ magnetic latitudes. We also indicate the day-night terminator at 110 km with the gray-dashed line.

The equivalent Sq current system on 9 August 2011 (Figure 5) shows the well-known current pattern with a counterclockwise vortex on the dayside of the Northern Hemisphere and a clockwise vortex on the dayside of the Southern Hemisphere. The snapshot of equivalent SFE current system (Figure 6) is also confined to the dayside. However, the current pattern is different from that of Sq. Multiple current cells can be seen in both Northern and Southern Hemispheres. The equivalent SFE current system represents the ionospheric current system superposed on the background Sq current system as fast as 3 min after the occurrence of the solar flare.

We also analyzed magnetic field data by SHA during the solar flare event of 24 September 2011, which occurred one and a half month after the first event. The pattern of the Sq current system shown in Figure 7 is similar to that in Figure 5, but the currents are somewhat stronger during the 24 September 2011 event. The SFE current system evolution in Figure 8 reveals a similar current pattern as the background Sq current system (Figure 7). The location of SFE current foci do not exactly agree with that of Sq current foci, as previously reported by Van Sabben (1961) and others.
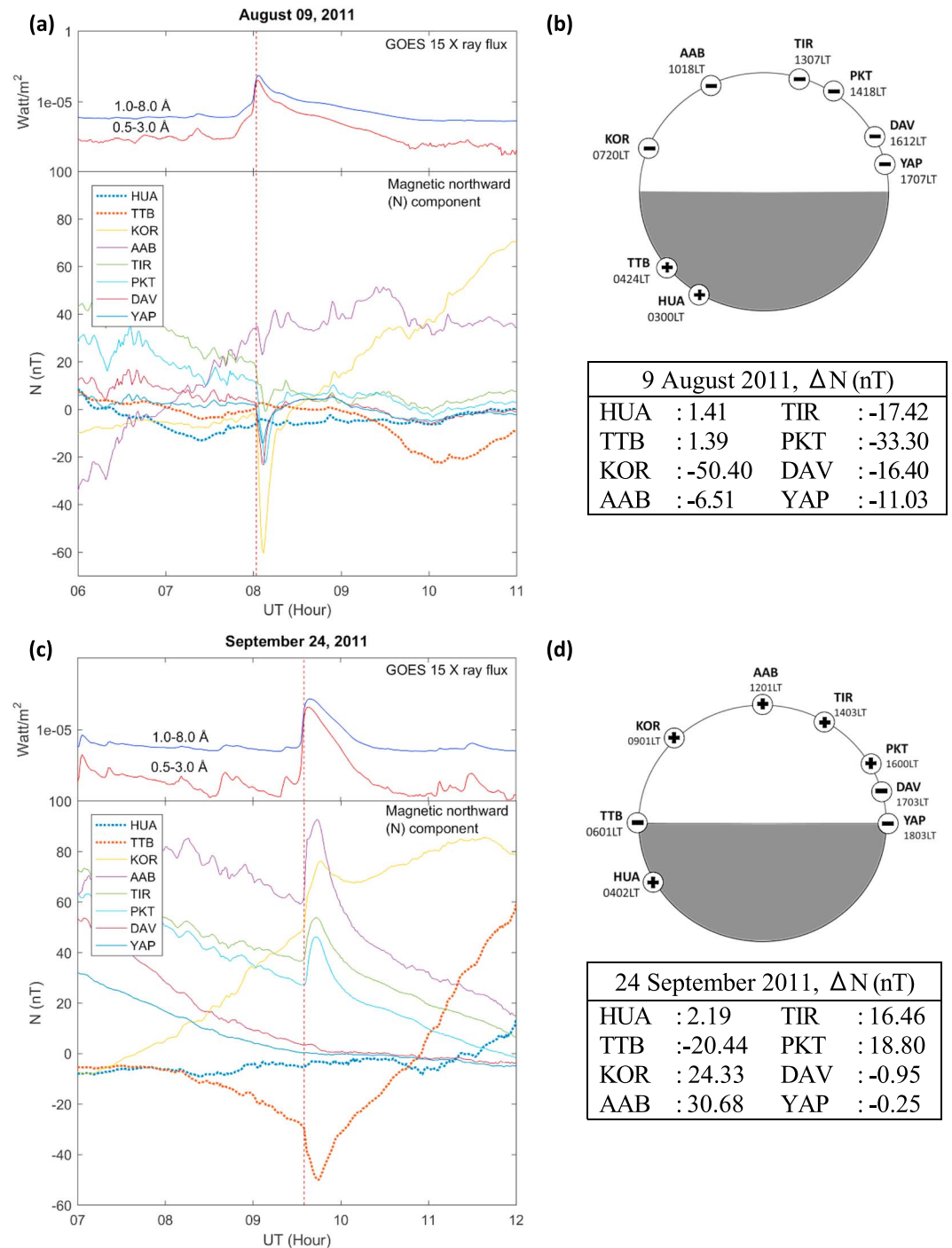
Figure 4. (a) Solar X-ray intensity and N-component magnetic field variations at equatorial stations during the solar flare event of 9 August 2011. (b) Location of the equatorial stations during the solar flare event. (c) and (d) are the same as (a) and (b), respectively, but for the solar flare event of 24 September 2011.

The results for the 24 September 2011 event confirm the known features of the SFE current system. The similarity between the SFE and Sq current systems suggests that the enhancement of the background Sq current system is the main cause of SFE currents, supporting earlier results in the literature (McNish, 1937, and many others). The present study demonstrated that the SFE current system is different in pattern from the background Sq current system during the 9 August 2011 event, in which SFE*s were

AGU
100
ADVANCING EARTH
AND SPACE SCIENCE

Journal of Geophysical Research: Space Physics

10.1029/2018JA025601
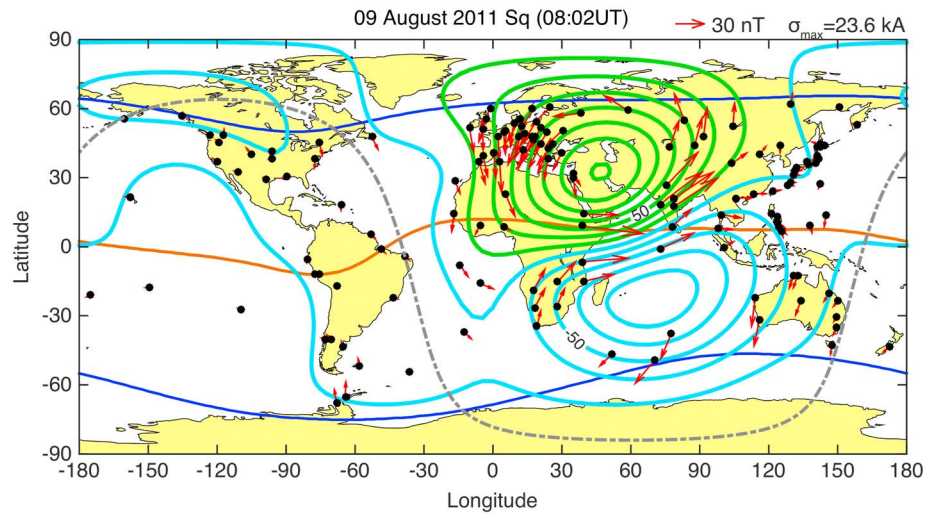
Figure 5. Equivalent ionospheric current systems for Sq before the X6.9 solar flare event on 9 August 2011.

observed at several dayside equatorial stations spread over a wide range of longitudes. Previous studies were not able to address the global ionospheric current system associated with SFE* due to the lack of data (Rastogi et al., 2013; Yamazaki et al., 2009). We have overcome this issue by using a large number of ground-based magnetometers and revealed for the first time the global structure of the current system.
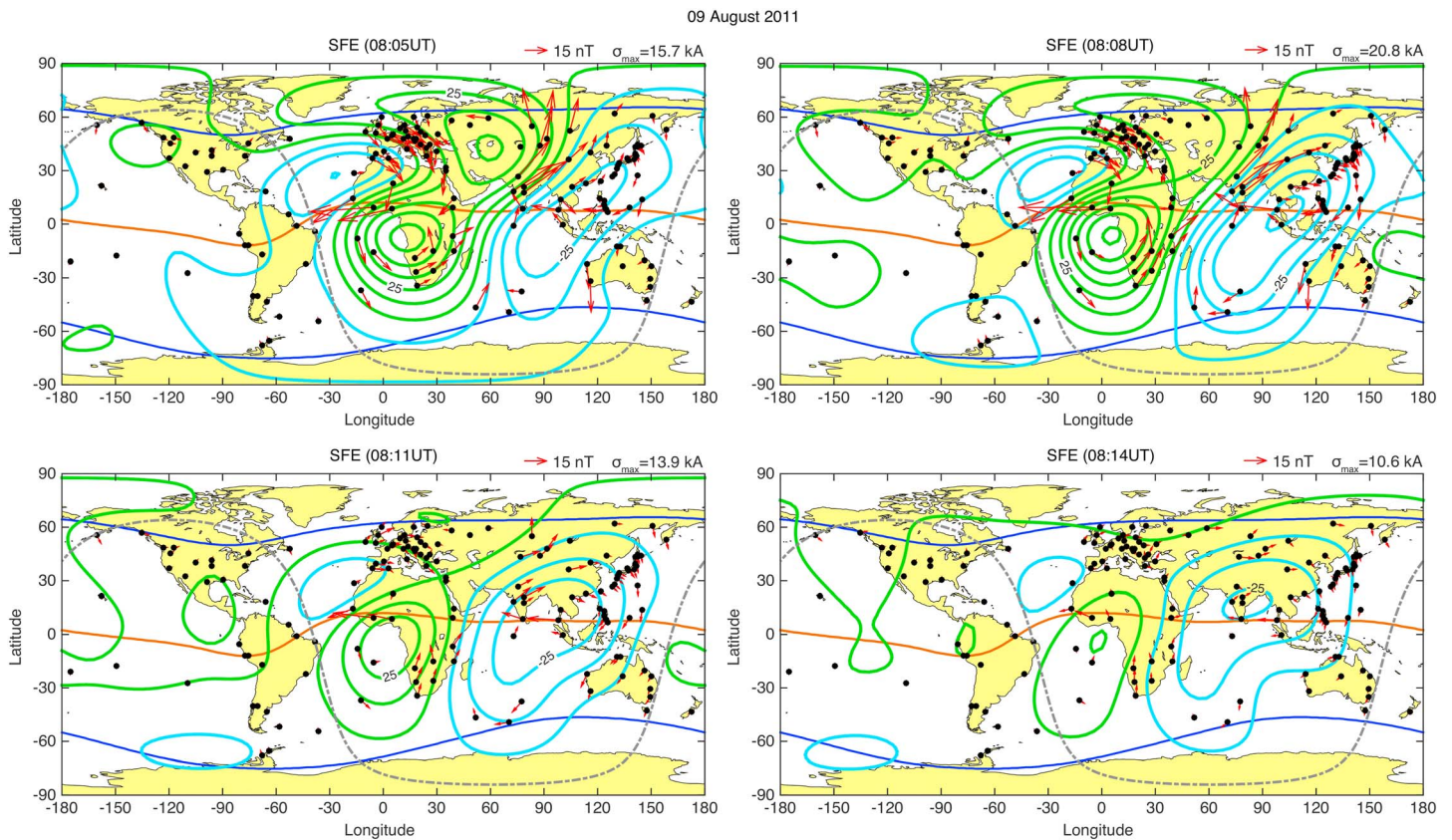
Figure 6. Snapshots of equivalent ionospheric current systems for SFE during the X6.9 solar flare event on 9 August 2011. SFE = solar flare effect.
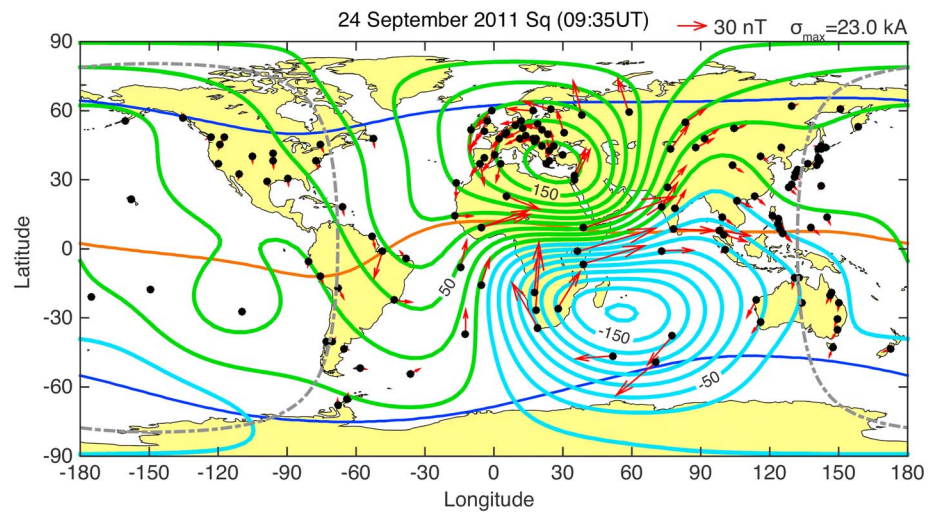
Figure 7. Same as Figure 5 except for the X1.4 solar flare event on 24 September 2011.

The reason for the unusual response of the ionosphere during the 9 August 2011 event is yet to be understood. The fact that the event occurred under quiet geomagnetic activity conditions rules out the effect of disturbance electric fields as suggested by Abdu et al. (2017). Recently, Zhang et al. (2017) showed that the equatorial electric field can be disturbed during solar flare events. It needs to be clarified how the global electric field responds during SFE* events.
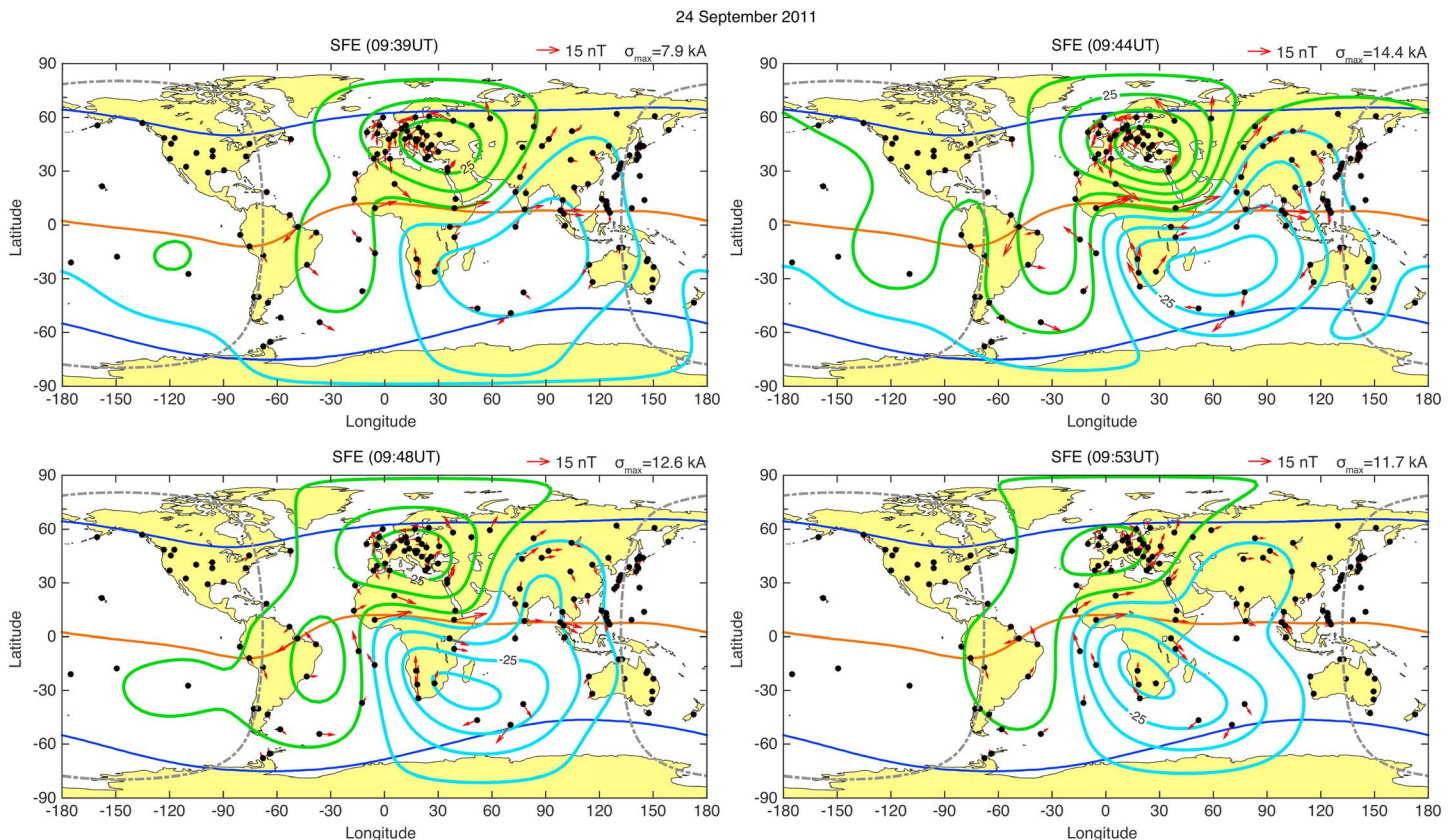
Figure 8. Same as Figure 6 except for the X1.4 solar flare event on 24 September 2011. SFE = solar flare effect.

The solar flare on 9 August 2011 was an X-class (X6.9) event, like other SFE* events previously reported. The SFE* events studied by Yamazaki et al. (2009) and Rastogi et al. (2013) were observed on 18 June 2000 (X1.0) and 3 July 2002 (X1.5). An intense X-class flare might be a necessary condition for SFE* to occur. Another common factor for these SFE* events is that they were all observed during the Northern-Hemisphere summer during days with Kp ≤ 3, which could also be a favorable condition for SFE*.

The different current patterns observed between Sq and SFE during the 9 August 2011 event suggest that the two current systems might be at different height regions. One possible candidate is the ionospheric D region below 90 km. As stated earlier, the X-ray in the 2–10-Å range can effectively ionize D-region heights. Indeed, ionosonde observations revealed evidence of enhanced D-region ionization during the 9 August 2011 event, as reported by Sripati et al. (2013). However, little is known about the D-region current system, and it is unclear whether the global current system shown in Figure 6 has any resemblance with the D-region current system. Another possible source is interhemispheric field-aligned currents (IHFACs) that flow from one hemisphere to the other at middle and low latitudes (Lühr et al., 2015; Park et al., 2011). The north-south asymmetry of the ionospheric conductivity, which might be enhanced during solar flare events, could drive IHFACs. However, the response of IHFACs to solar flares is unknown.

4. Conclusions

We have examined the geomagnetic crochets due to the X-class solar flare on 9 August 2011 (X6.9) and 24 September 2011 (X1.9) using extensive ground-based magnetometer observations. The equivalent ionospheric current systems were evaluated based on a SHA for both cases, and the two results were compared. Main findings of this study are summarized below.

1. There is a significant difference in the response of equatorial ionospheric currents between the two events. During the 9 August 2011 event, negative crochets were observed in the magnetic northward (N) component at all the dayside equatorial stations. SFE*s (i.e., counter-Sq SFEs) were detected at five stations in the local time sectors 10:18–17:07 LT. In contrast, the daytime eastward EEJ was observed to enhance during the 24 September 2011 event.
2. The results of the SHA, involving magnetic data from nearly 160 stations, shows that the global pattern of the ionospheric SFE current system was totally different from that of the background Sq current system during the 9 August 2011 event, while the SFE current system was similar in pattern with the background Sq current system during the 24 September 2011 event.
3. The difference in the global pattern of the SFE and Sq current systems during the 9 August 2011 event suggests that the ionospheric currents associated with SFE* may not flow mainly in the E region as Sq currents. Contribution from the D region is suspected from the previous ionosonde observation by Sripati et al. (2013).

References

Abdu, M. A., Nogueira, P. A. B., Souza, J. R., Batista, I. S., Dutra, S. L. G., & Sobral, J. H. A. (2017). Equatorial electrojet responses to intense solar fares under geomagnetic disturbance time electric fields. *Journal of Geophysical Research: Space Physics*, 122, 3570–3585. https://doi.org/10.1002/2016JA023667

Alken, P., Chulliat, A., & Maus, S. (2013). Longitudinal and seasonal structure of the ionospheric equatorial electric field. *Journal of Geophysical Research: Space Physics*, 118, 1298–1305. https://doi.org/10.1029/2012JA018314

Annadurai, N. M. N., N.S.A, H., & A, Y. (2018). Pemerhatian Arus Ionosfera semasa Suar Suria Kuat menggunakan Data Magnetometer Dasar. *Sains Malaysiana*, 47(3), 595–601. https://doi.org/10.17576/jsm-2018-4703-21

Baker, W. G., & Martyn, D. F. (1953). Electric currents in the ionosphere—The conductivity. *Philosophical Transactions of the Royal Society A*, 246(913), 281–294. https://doi.org/10.1098/rsta.1953.0016

Campbell, W. H. (2003). *Introduction to geomagnetic fields*. Cambridge: Cambridge University Press.

Chapman, S. (1951). The equatorial electrojet as detected from the abnormal electric current distribution above Huancayo, Peru, and elsewhere. *Archiv für Meteorologie, Geophysik und Bioklimatologie Serie A*, 4(1), 368–390. https://doi.org/10.1007/BF02246814

Chulliat, A., Vigneron, P., & Hulot, G. (2016). First results from the Swarm dedicated ionospheric field inversion chain. *Earth, Planets and Space*, 68(1), 104. https://doi.org/10.1186/s40623-016-0481-6

Curto, J. J., Amory-Mazaudier, C., Torta, J. M., & Menvielle, M. (1994). Solar flare effects at Ebre: Unidimensional physical, integrated model. *Journal of Geophysical Research*, 99(A12), 23289–23296. https://doi.org/10.1029/94JA02070

Gaya-Piqué, L. R., Curto, J. J., Torta, J. M., & Chulliat, A. (2008). Equivalent ionospheric currents for the 5 December 2006 solar flare effect determined from spherical cap harmonic analysis. *Journal of Geophysical Research*, 113, A07304. https://doi.org/10.1029/2007JA012934

Gjerloev, J. W. (2009). A global ground-based magnetometer initiative. *Eos, Transactions American Geophysical Union*, 90(27), 230–231. https://doi.org/10.1029/2009EO270002

Gjerloev, J. W. (2012). The SuperMAG data processing technique. *Journal of Geophysical Research*, *117*, A09213. https://doi.org/10.1029/2012JA017683

Hamid, N. S. A., Liu, H., Uozumi, T., Yumoto, K., Veenadhari, B., Yoshikawa, A., & et al. (2014). Relationship between the equatorial electrojet and global Sq currents at the dip equator region. *Earth, Planets and Space*, *66*(1), 146. https://doi.org/10.1186/s40623-014-0146-2

Hirono, M. (1950). On the influence of the Hall current to the electrical conductivity of the ionosphere. I. *Journal of Geomagnetism and Geoelectricity*, *2*(1), 1–8. https://doi.org/10.5636/jgg.2.1

Huang, C.-M., Richmond, A. D., & Chen, M.-Q. (2005). Theoretical effects of geomagnetic activity on low-latitude ionospheric electric fields. *Journal of Geophysical Research*, *110*, A05312. https://doi.org/10.1029/2004JA010994

Laundal, K. M., & Richmond, A. D. (2017). Magnetic coordinate systems. *Space Science Reviews*, *206*(1–4), 27–59. https://doi.org/10.1007/s11214-016-0275-y

Love, J. J., & Chulliat, A. (2013). An international network of magnetic observatories. *Eos, Transactions American Geophysical Union*, *94*(42), 373–374. https://doi.org/10.1002/2013EO420001

Lühr, H., Kervalishvili, G., Michaelis, I., Rauberg, J., Ritter, P., Park, J., et al. (2015). The interhemispheric and F region dynamo currents revisited with the Swarm constellation. *Geophysical Research Letters*, *42*, 3069–3075. https://doi.org/10.1002/2015GL063662

Marriott, R. T., Richmond, A. D., & Venkateswaran, S. V. (1979). The quiet-time equatorial electrojet and counter-electrojet. *Journal of Geomagnetism and Geoelectricity*, *31*(3), 311–340. https://doi.org/10.5636/jgg.31.311

Maruyama, T., Kawamura, M., Saito, S., Nozaki, K., Kato, H., Hemmakorn, N., et al. (2007). Low latitude ionosphere-thermosphere dynamics studies with ionosonde chain in Southeast Asia. *Annales de Geophysique*, *25*(7), 1569–1577. https://doi.org/10.5194/angeo-25-1569-2007

Matsushita, S. (1965). Global presentation of the external Sq and L current systems. *Journal of Geophysical Research*, *70*(17), 4395–4398. https://doi.org/10.1029/JZ070i017p04395

Matsushita, S., & Xu, W. Y. (1982). Equivalent ionospheric current systems representing solar daily variations of the polar geomagnetic field. *Journal of Geophysical Research*, *87*(A10), 8241–8254. https://doi.org/10.1029/JA087iA10p08241

Mayaud, P. N. (1977). Equatorial counter-electrojet—A review of its geomagnetic aspects. *Journal of Atmospheric and Solar - Terrestrial Physics*, *39*(9–10), 1055–1070. https://doi.org/10.1016/0021-9169(77)90014-9

McNish, A. G. (1937). Terrestrial, magnetic and ionospheric effects associated with bright chromospheric eruptions. *Terrestrial Magnetism and Atmospheric Electricity*, *42*(2), 109–122. https://doi.org/10.1029/TE042i002p00109

Nagata, T. (1952). Characteristics of the solar flare effect (Sqa) on geomagnetic field at Huancayo (Peru) and at Kakioka (Japan). *Journal of Geophysical Research*, *57*(1), 1–14. https://doi.org/10.1029/JZ057i001p00001

Park, J., Lühr, H., & Min, K. W. (2011). Climatology of the inter-hemispheric field-aligned current system in the equatorial ionosphere as observed by CHAMP. *Annales de Geophysique*, *29*(3), 573–582. https://doi.org/10.5194/angeo-29-573-2011

Rahim, Z., & Kumbher, A. S. (2016). Solar daily variation at geomagnetic observatories in Pakistan. *Journal of Atmospheric and Solar - Terrestrial Physics*, *140*, 41–54. https://doi.org/10.1016/j.jastp.2016.01.016

Rastogi, R. G. (1974). Westward equatorial electrojet during daytime hours. *Journal of Geophysical Research*, *79*, 1503–1512. https://doi.org/10.1029/JA079i010p01503

Rastogi, R. G., Chandra, H., & Yumoto, K. (2013). Unique examples of solar flare effects in geomagnetic H field during partial counter electrojet along CPMN longitude sector. *Earth, Planets and Space*, *65*(9), 1027–1040. https://doi.org/10.5047/eps.2013.04.004

Rastogi, R. G., Deshpande, M. R., & Sastri, N. S. (1975). Solar flare effect in equatorial counter electrojet currents. *Nature*, *258*(5532), 218–219. https://doi.org/10.1038/258218a0

Rastogi, R. G., Pathan, B. M., Rao, D. R. K., Sastry, T. S., & Sastri, J. H. (1999). Solar flare effects on the geomagnetic elements during normal and counter electrojet periods. *Earth, Planets and Space*, *51*(9), 947–957. https://doi.org/10.1186/BF03351565

Richmond, A. D. (1995). Ionospheric electrodynamics. In H. Volland (Eds.), *Handbook of Atmospheric Electrodynamic* (Vol. 2, pp. 249–290). Boca Raton, FL: CRC Press.

Richmond, A. D., & Maute, A. (2014). Ionospheric electrodynamics modeling. In J. Huba, R. Schunk, & G. Khazanov (Eds.), *Modeling the Ionosphere-Thermosphere System*. Chichester, UK: John Wiley. https://doi.org/10.1002/9781118704417.ch6

Richmond, A. D., & Venkateswaran, S. V. (1971). Geomagnetic crochets and associated ionospheric current systems. *Radio Science*, *6*(2), 139–164. https://doi.org/10.1029/RS006i002p00139

Sastri, J. H. (1975). The geomagnetic solar are of 6 July 1968 and its implications. *Annales de Geophysique*, *31*, 481–485.

Shimizu, H., & Utada, H. (1999). Ocean hemisphere geomagnetic network: Its instrumental design and perspective for long-term geomagnetic observations in the Pacific. *Earth, Planets and Space*, *51*(9), 917–932. https://doi.org/10.1186/BF03351563

Sripati, S., Balachandran, N., Veenadhari, B., Singh, R., & Emperumal, K. (2013). Response of the equatorial and low-latitude ionosphere to an intense X-class solar flare (X7/2B) as observed on 09 August 2011. *Journal of Geophysical Research: Space Physics*, *118*, 2648–2659. https://doi.org/10.1002/jgra.50267

Takeda, M. (1999). Time variation of global geomagnetic Sq field in 1964 and 1980. *Journal of Atmospheric and Solar - Terrestrial Physics*, *61*(10), 765–774. https://doi.org/10.1016/S1364-6826(99)00028-0

Takeda, M. (2002). Features of global geomagnetic Sq field from 1980 to 1990. *Journal of Geophysical Research*, *107*(A9), 1252. https://doi.org/10.1029/2001JA009210

Thome, G. D., & Wagner, L. S. (1971). Electron density enhancements in the E and F regions of the ionosphere during solar flares. *Journal of Geophysical Research*, *76*(28), 6883–6895. https://doi.org/10.1029/JA076i028p06883

Van Sabben, D. (1961). Ionospheric current systems of ten IGY-solar flare effects. *Journal of Atmospheric and Terrestrial Physics*, *22*(1), 32–42. https://doi.org/10.1016/0021-9169(61)90175-1

Van Sabben, D. (1968). Solar flare effects and simultaneous magnetic daily variation, 1959–1961. *Journal of Atmospheric and Terrestrial Physics*, *30*(9), 1641–1648. https://doi.org/10.1016/0021-9169(68)90012-3

Veldkamp, J., & Van Sabben, D. (1960). On the current system of solar flare effects. *Journal of Atmospheric and Terrestrial Physics*, *18*(2–3), 192–202. https://doi.org/10.1016/0021-9169(60) 90092-1

Weimer, D. R. (2013). An empirical model of ground-level geomagnetic perturbations. *Space Weather*, *11*, 107–120. https://doi.org/10.1002/swe.20030

Yamazaki, Y., & Maute, A. (2017). Sq and EEJ—A review on the daily variation of the geomagnetic field caused by ionospheric dynamo currents. *Space Science Reviews*, *206*(1–4), 206–299. https://doi.org/10.1007/s11214-016-0282-z

Yamazaki, Y., Yumoto, K., Cardinal, M. G., Fraser, B. J., Hattori, P., Kakinami, Y., et al. (2011). An empirical model of the quiet daily geomagnetic field variation. *Journal of Geophysical Research*, *116*, A10312. https://doi.org/10.1029/2011JA016487

Yamazaki, Y., Yumoto, K., Yoshikawa, A., Watari, S., & Utada, H. (2009). Characteristics of counter-Sq SFE (SFE*) at the dip equator CPMN stations. *Journal of Geophysical Research*, *114*, A05306. https://doi.org/10.1029/2009JA014124

Yasuhara, M., & Maeda, H. (1961). Geomagnetic crochet of 15 November 1960. *Journal of Atmospheric and Terrestrial Physics*, *21*(4), 289–293. https://doi.org/10.1016/0021-9169(61)90164-7

Yumoto, K., and the MAGDAS Group (2006), MAGDAS project and its application for space weather, in *36th COSPAR Scientific Assembly,* 36.

Zhang, R., Liu, L., Le, H., & Chen, Y. (2017). Equatorial ionospheric electro- dynamics during solar flares. *Geophysical Research Letters*, *44*, 4558–4565. https://doi.org/10.1002/2017GL073238